Feasibility study of new metrology for x-ray capillary development

Brenden Roberts*
Laboratory for Elementary Particle Physics, Cornell University, Ithaca, NY, 14850
Advisors: Dr. Rong Huang, Dr. Peter Revesz

August 14, 2012

Abstract

A new system has been proposed for realtime monitoring of the inner diameter (ID) of an x-ray capillary during the pulling process. The system relies on an ultraviolet LED shining light through the capillary. Monte Carlo raytracing simulations indicate that for the duration of the capillary pull, a linear relationship exists between the minimum radius and the observed light transmission ratio. This relationship is unaffected by bends in the capillary of up to 50 μm or typical diameter errors. Experiments performed using preexisting glass tubes confirm these results; thus, it will be possible to implement this metrology into the capillary pulling process. The raytracer developed for this project is the first fully 3D capillary raytracing code written at Cornell, and can be easily adapted to simulate x-ray focusing by capillaries.

Contents

*Department of Physics & Astronomy, Clemson University, Clemson, SC 29634

1 Introduction to synchrotron radiation

The synchrotron is one of the foremost devices used to generate high-energy x-rays. For decades, researchers have accelerated beams of electrons and positrons in order to generate electromagnetic radiation at energies unreachable for lower-powered machines. The Cornell Electron Storage Ring (CESR) provides the beam for the Cornell High Energy Synchrotron Source (CHESS) project. Researchers use this facility to perform many experimental techniques, among which are x-ray diffraction and x-ray fluorescence.

The principle underlying synchrotron radiation is simply that charged particles radiate when accelerated. The energy of the emitted radiation is dependent upon that of the beam and the device used to generate the radiation, and is in the high-energy x-ray range for CESR. Because the particles in a storage ring are moving at relativistic speeds, the radiation—which would otherwise emanate in a spherical wave, as from a point source—is released in a narrow cone centered in the direction of travel. If a bending magnet (used to maintain the beam's circular path in a storage ring) is the source, the radiation cone is tangential to the ring and its angular opening is given by

$$\theta_r = \frac{1}{\gamma}, \tag{1}$$

where γ is the Lorentz factor of the beamline [1, p. 11]. The bandwidth and spatial distribution is not immediately useful for performing x-ray experiments, so crystals and mirrors are used to monochromatize or focus the beam, respectively, upstream of microfocusing devices, such as a capillary, which performs the final focusing before the x-rays reach a sample.

2 X-ray capillaries

2.1 Motivation

Many types of x-ray focusing devices exist, for a variety of experimental applications. Many are designed to handle the so-called "white" beam coming directly from a synchrotron. These often either provide some focusing in one axis or select a certain bandwidth of x-ray to pass to other, more sensitive optics. The monochromators are often be composed of two large crystals and employ the principle of Bragg reflection, and the focusers are often simply slightly curved mirrors [1, p. 24]. However, optical devices like these cannot perform all of the focusing necessary for micro- or nanoscale x-ray experiments. To shape the beam into its final, usable form, microfocusing optics are required.

These microfocusing optics are characterized by their reliance on the principle of *total external reflection*, a behavior unique to the x-ray energy range. Within this region, refractive indices are given by

$$n = 1 - \delta - i\beta, \tag{2}$$

where δ is approximately on the order of 10^{-5} for glass. The imaginary part β is more variable but is often several orders of magnitude smaller than δ and represents an attenuation factor of photons in the material. As a consequence, instead of total internal reflection—as occurs for visible light

in a fiber optic cable—x-rays experience total external reflection. Because n is very close to 1, the critical angle is extremely low. For glass, it can be approximated by [1, p. 42]

$$\theta_c \approx \frac{32}{E_c}, \tag{3}$$

with θ_c given in mrad and E_c in keV. Thus a 10 keV x-ray has a critical angle of only 3.2 mrad, slightly less than 0.2°. Below the critical angle, these materials act like a mirror, reflecting almost all intensity. At angles higher than θ_c, there is almost no reflection.

The primary type of microfocusing optic in use at CHESS is the *single-bounce monocapillary* (SBMC), which were the specific subject of this REU project. The idea behind their design is that rays emanating from the focus of an ellipse will reflect off of its boundary exactly once and then arrive at the other focus. Accordingly, the shape of an SBMC is a glass ring fitted to a very small section of an ellipsoid with extremely high eccentricity. The semimajor axis of this ellipsoid is often of the order of 10 m, whereas the semiminor axis is $\leq$1 mm. The x-ray source is located at one of the elliptical foci and the other is the optical focus. A beamstop prevents any direct rays from saturating the working area with unwanted noise. This profile shape provides a number of benefits: ideal cases are capable of achieving focal spot sizes around or less than 50 μm with gains on the order of 10^3. Additionally, because x-rays reflect only once, below the critical angle, the capillary acts like an optical fiber and reaches almost 100% optical efficiency. SBMC's are also achromatic; different wavelengths of x-ray are focused at the same point, as a necessity of the elliptical profile. Thus a specific focal distance can be built into the capillary shape during construction to suit a particular purpose.

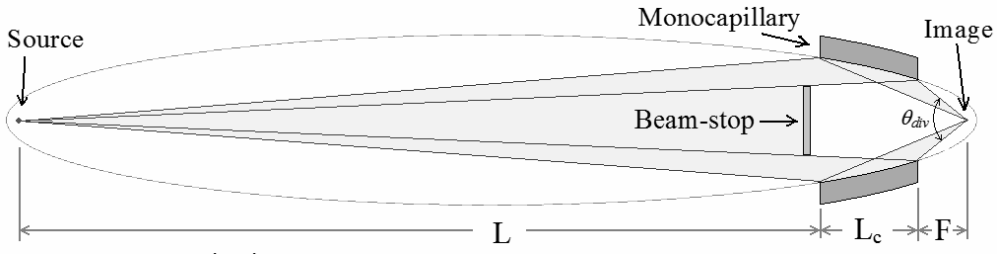

Figure 1: Single-bounce monocapillary illustration [1, p. 43]

2.2 Construction techniques

The exact specifications of the shape of a capillary are given by the parameters indicated in Figure 1: viz., the distance to the source, L; the length of the capillary, L_c; the focal length, F; the maximum divergence θ_{div}; and others. A challenge inherent to this design is that the capillaries must be constructed to fit this nominal profile with a high degree of precision, or the focusing will be ineffective. To perform this task, CHESS uses a *capillary pulling machine*. The machine itself consists of a vertical stage to which a straight glass tube can be attached at both ends by strings. The tube sits inside a small mobile furnace which can move along the length of the tube, heating the glass at any point. Variable tension can be applied to the tube ends via the strings. The furnace

heats the tube starting at the top, and the tension causes the melted glass to stretch, shrinking the inner and outer diameters in the heated area in order to satisfy conservation of mass. The action of the furnace is what governs the shape being created; the furnace itself is guided by a preprogrammed routine designed to pull the tube into the desired ideal profile.

2.3 Proposed metrology system

The current capillary pulling strategy described in Section 2.2 provides reasonable control and accuracy. However, it gives no source of real-time feedback during a capillary pull. In the ideal case, this would not be problematic, but real glass tubes come with a variety of inherent errors: *centerline deflection* refers to the "banana"-curvature of a tube along its length, *diameter error* describes the many small deviations of the inner shape from the ideal cylinder, and many tubes also display an inner *periodic ripple*. It is possible that a combination of these factors can render a seemingly appropriate pulling program useless. Realtime feedback would allow one to know the minimum radius of the capillary during the entirety of the pulling process and adjust the furnace strategy on-the-fly to account for all of these capillary defects.

The proposed way to determine this radius information is simple: shine an ultraviolet light down the tube during the pull and measure the intensity of transmitted light at the other end with a photodiode filtered to only accept UV wavelengths. *Evaluating this strategy is the overall focus of my REU project.* Ultraviolet light was selected, as opposed to visible, for two reasons:

1. UV light is close to x-rays in reflectance
2. Glass tubes are opaque to UV but transparent to visible light

The first point simply acknowledges that in an optic designed for x-rays, using similar frequencies will likely yield the best measurement results. As for the second, if visible light were used all of the intensity would pass through the glass of the tube walls without any attenuation and there would be no difference in readings for the beginning and ending pull stages. Ultraviolet rays see glass as primarily opaque and thus reflects well off of it. Therefore UV light provides an ideal choice; the majority of the observed light at the end of the capillary should be that which has passed directly through the opening, with the rest reflecting off of the walls and not reaching the end.

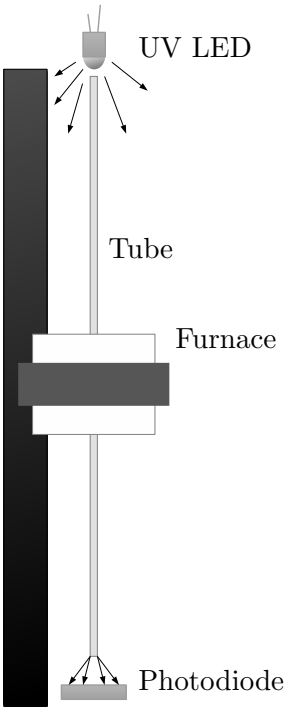

Figure 2: Proposed measurement system, shown installed on puller

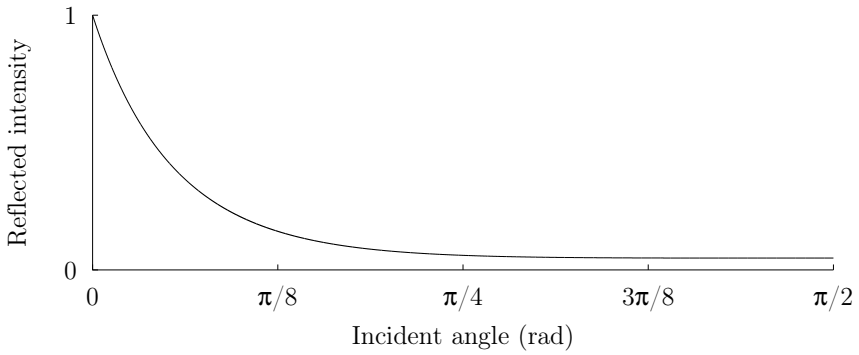

Figure 3: UV reflectance for glass

3 Numerical simulations

The primary objective of this project was to simulate the proposed LED-capillary system in order to establish its expected efficacy. The simulation itself comprises formulas for generating a numerical representation of any given capillary, as well as code using a Monte Carlo raytracing algorithm to model light propagation. An overview of my simulation's methods follows. For an exhaustive description of the mathematics involved, one may refer to the source code documentation.

3.1 Raytracing code overview

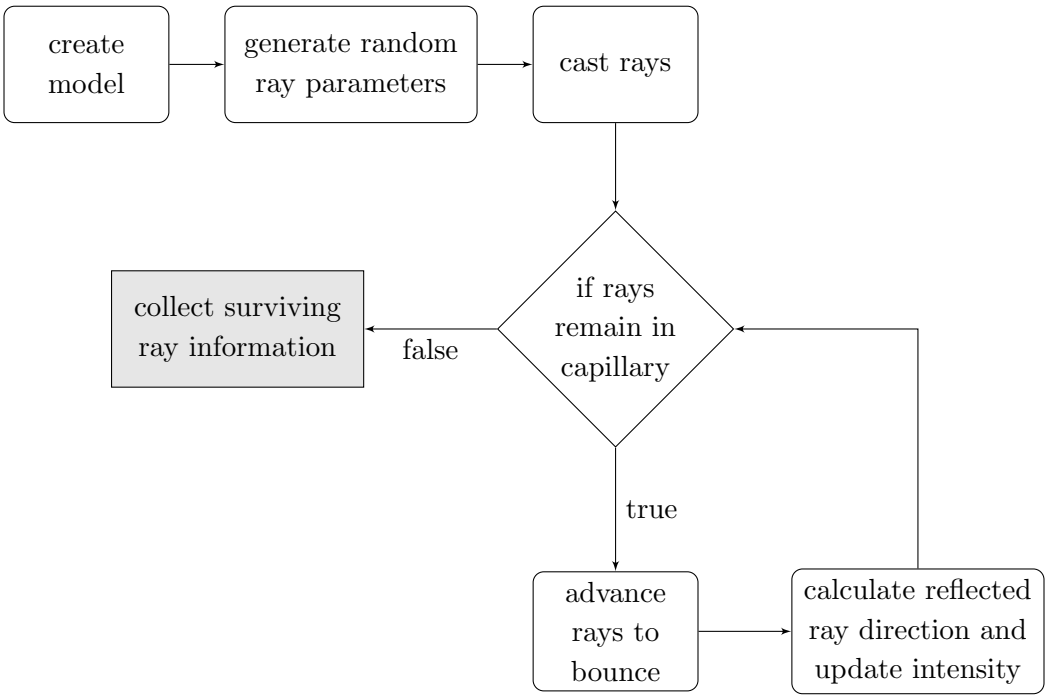

Figure 4: Raytracer logical layout

The first step in the process is to create a model of a capillary for use by the simulation code. It is this model which allows the program to ascertain the particular point at which a ray intersects the capillary wall. In order to generate this model, the program must be given various parameters related to the specific usage of the capillary; among these are, for instance, the desired focal distance, maximum allowed divergence, and source distance. From this list the ideal capillary shape is calculated using formulas adapted from a paper by Rong Huang [2]. This ideal profile has two types of error introduced to it: centerline deflection, which is preprogrammed in the capillary shape, and diameter error, which refers to random (non-deterministic) perturbations of the actual shape off of the ideal value.

Centerline deflection refers to the overall bend of the capillary along its length. It is expected that much of the light observed to have been transmitted through the capillary will have passed directly through the capillary without encountering any of the walls. Thus if the capillary is bent to such an extent that the point of minimum radius is occluded by the ends, one would expect a drop in transmission proportional to the area. Typical bending values are 5 μm–40 μm. In contrast, diameter error affects the light that does encounter the capillary wall; by introducing randomness into the profile, reflections are not necessarily as efficient as in an ideal capillary and so less of the reflected light passes through the capillary. Unmelted portions of the profile have roughly an RMS diameter error of 5 μm while shaped portions have RMS error 1 μm.

The use of raytracing code to perform simulations of capillary optic behavior is widely-practiced. While programs with very similar feature sets to that of my project have been implemented elsewhere [3], this is the first fully three-dimensional capillary raytracing code written at Cornell. The concept has been implemented previously, but only in two dimensions. Prior 2D simulations were capable of providing some insight into the behavior of light in a capillary, but this represents a significant jump in the predictive power of this type of program. A *2D simulation* refers to taking a planar "slice" axially through the center of a capillary, and modeling the rays as if they moved only in this space. It is notable that in such a simulation, the area available to the rays scales linearly with radius, as r, whereas 3D rays act in a volume which scales as r^2. Additionally, if one only considers a slice through the center of a capillary, many rays which do not happen to fully lie in this plane must be ignored or somehow projected into the space, and a wide range of reflection behavior at glancing angles cannot be captured.

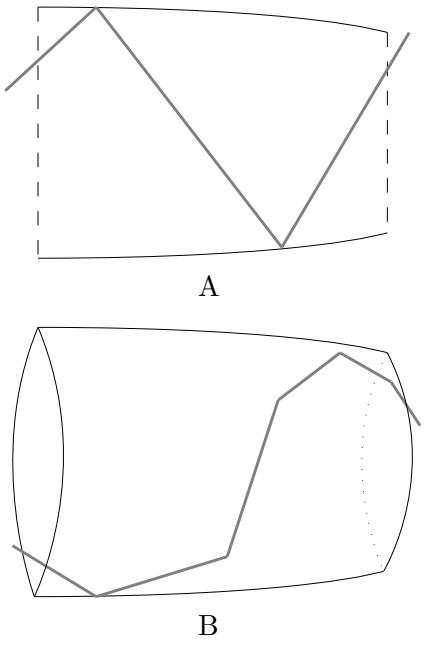

Figure 5: 2D (A) and 3D (B) models.

Within the capillary, rays travel in a straight path without any attenuation of intensity. When any particular ray has intersected the wall of the capillary, the normal vector to the wall at the point of contact is found by using the cross-product of gradients. If $f(r, \varphi, z)$ is the function representing

the capillary wall, then based on the definition of the gradient and cross product, the unit normal is [3]

$$\vec{n} = \frac{\frac{\partial f}{\partial \varphi} \times \frac{\partial f}{\partial z}}{\| \frac{\partial f}{\partial \varphi} \times \frac{\partial f}{\partial z} \|}. \tag{4}$$

Using the unit normal $\vec{n}$ and the initial ray direction $\vec{u_i}$, one can find the reflected ray direction $\vec{u_r}$ easily using the reflection formula

$$\vec{u_r} = \vec{u_i} - 2(\vec{u_i} \cdot \vec{n})\vec{n}. \tag{5}$$

In addition to updating the ray's propagation information, its intensity must also be monitored. Every time it reflects, its outgoing intensity is attenuated by a factor $R < 1$, which is determined by the angle of intersection of the beam, θ_i, the wavelength (for UV light, $n \approx 1.55 + 6.33 \times 10^{-5} i$), and the polarization of the light relative to the surface.

$$I = RI_0 \tag{6}$$

For unpolarized light, R is the average of the parallel value $R_\parallel$ and perpendicular $R_\perp$:

$$R_\parallel = \frac{n^2 \cos\theta_i - i\sqrt{\sin^2\theta_i - n^2}}{n^2 \cos\theta_i + i\sqrt{\sin^2\theta_i - n^2}} \tag{7}$$

$$R_\perp = \frac{\cos\theta_i - i\sqrt{\sin^2\theta_i - n^2}}{\cos\theta_i + i\sqrt{\sin^2\theta_i - n^2}} \tag{8}$$

After enough bounces at sufficiently high angles, a ray becomes so faint that its contribution to the total flux leaving the tube is negligible. To improve simulation speed, such rays are discarded once they reach a certain threshold; in most simulations without significant bending or distortion, a threshold of 0.001 of the initial intensity is sufficiently low.

Once the insignificant rays have been eliminated and the others have passed fully through the tube, this information can be handled in several ways. Most simply, one can take the integral of the transmitted intensity, yielding a single number, and compare it to the initial intensity. This mimics a photodiode's behavior and thus was the primary method of analysis performed in this project. However, another option is to map the position of each ray, along with its intensity, at or beyond the capillary's end to generate a spatial distribution image. This mimics the recording behavior of a CCD and while this type of image was not strictly within the main focus of this project, they are very useful in other contexts and it is within the capacity of my raytracer to generate them. They are very useful as additional verification of the validity of a simulation, and several spatial plots are presented in the results section.

3.2 Negligible refraction assumption

One assumption that this raytracer relies on for its accuracy is that the intensity of light rays that refract through the inner wall of the capillary can be ignored; that is, none of these rays are

propagated through to the final calculation. There are some grounds for making this claim: while in the capillary wall, the photons will have their intensity attenuated exponentially with distance:

$$I(x) = I_0 e^{-\mu x}, \mu = \frac{4\pi}{\lambda_0} n_i, \tag{9}$$

where n_i is the imaginary part of the refractive index and λ_0 is the nominal wavelength. This by itself does not prove the assumption. A ray could conceivably refract into the wall, reflect off of the outer capillary wall after traveling a short distance, and refract back into the inner tube region where it would add to the measured intensity.

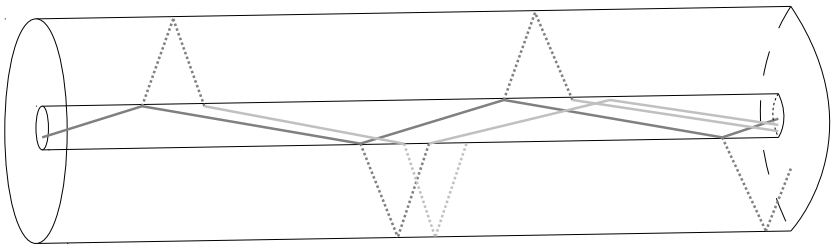

Figure 6: Illustration of refracted UV ray transmission

To demonstrate the validity of this assumption, a separate simulation had to be written. It utilized a recursive algorithm; instead of each ray being represented by a set of numbers inside a master program, each ray was itself a copy of this code which existed in the computer processor register. Each time an interface of media is encountered by a ray, not only does it reflect itself, but it also spawns a new copy of the program in memory with the appropriate position and direction of the refracted ray. This type of simulation is far more complicated to write and incredibly memory-intensive, especially in three dimensions, and thus a simple simulation with a short, ideal tube was performed. Even in the most ideal circumstances, it was found that these refracted rays contribute less than 1% of the final intensity and thus can be safely disregarded.

3.3 Runtime analysis

Raytracers are notorious in the field of computer science for being extremely slow algorithms, especially on CPUs or systems with few cores. Being comprised of many, relatively simple, calculations, they are prime subjects for parallel computation. However, that option was not available in the context of this project. Thus my raytracing code uses a very specific vectorized methodology. In contrast, a popular approach is to calculate the ray paths serially. To do this, one uses a large array of ray data and propagates each ray in its entirety before moving on to the next in the array. A parallel raytracer—distinct from a *parallelized* raytracer, which runs on multiple compute cores—casts all rays simultaneously, "shotgun" style. The improvement in calculation speed comes from the fact that the code is written in the MATLAB scripting language, which is heavily optimized for performing operations on entire matrices rather than the same number of calculations on discrete scalar values.

Both types of algorithm run in $\Theta(n)$ time; that is, the runtime for a given simulation is always proportional to n, the number of rays cast in the simulation, up to constant addition. Therefore the constant of proportionality is of concern, and can be seen to be drastically different for the two programs, approximately by a factor of 10.

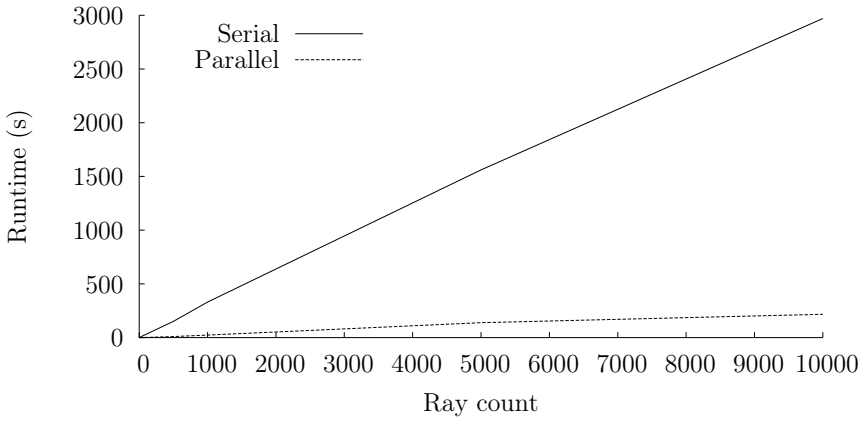

Figure 7: Serial vs. parallel runtime comparison

4 Simulation results

The simulation results are quite promising for the fundamental idea behind this metrology. It was expected that a linear trend would be seen in the measured UV light intensity at the far end of the capillary as a pull proceeds and this trend is clear, as seen in Figure 8.

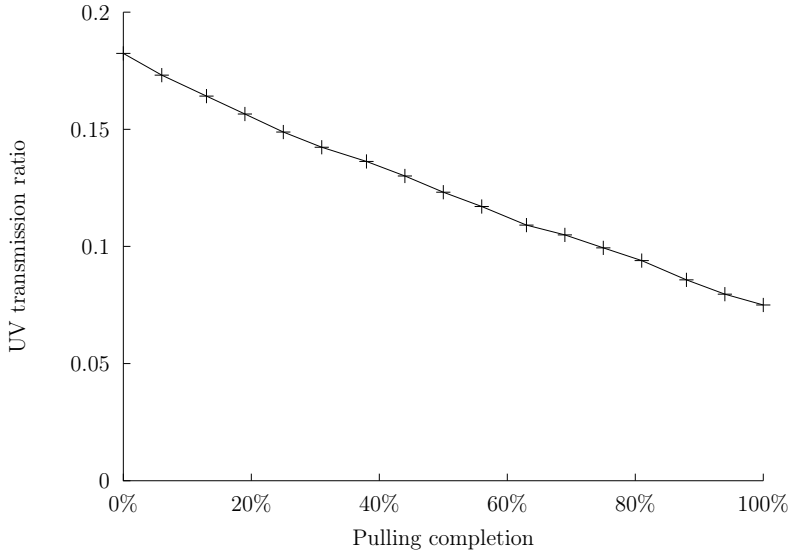

Figure 8: Simulated straight capillary UV transmission

The capillary profile used for this calculation had a maximum radius of 0.4 mm, a minimum radius of 0.12 mm, and an initial tube length of 20 cm.

4.1 Centerline deflection effects

It was of concern to what extent preexisting capillary centerline deflection would affect the simulation results. With the same capillary parameters as before, it can be seen in Figure 9 that up to at least around 40% of the capillary minimum radius, bending has absolutely no effect on the observations.

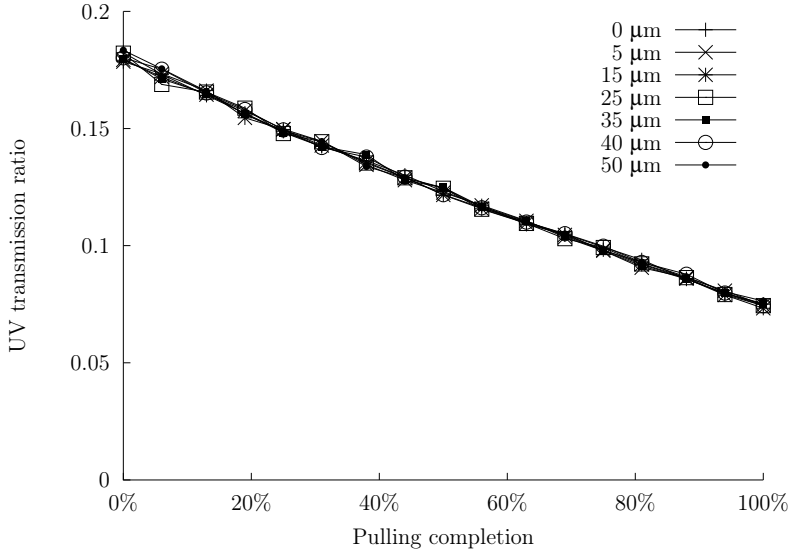

Figure 9: Simulated straight capillary UV transmission, with centerline deflections

4.2 Spatial distribution

It is also possible to generate spatial plots, in which the distribution of the transmitted intensity is visible. For the purposes of the project, the integral over the whole area is of greater concern, but it is important that the outward-bound rays be well-behaved so that they can be easily collected. These plots help one determine the required photodiode size in order to view the entire spot, based on the distance from the tube.

The spatial plots were generated from a relatively short capillary simulation with a maximum inner radius of 0.5 mm; longer capillaries result in fewer indirect rays, and thus there is less of a difference between close and far distances. Figure 10 shows the distribution 1 mm away from the capillary end; this is before rays have a chance to spread, and they are all clustered in the area at the inner region of the tube. Figure 11 is plotted on the same scale as Figure 10 but at a distance of 10 mm from the capillary end and shows a marked Gaussian dispersion pattern, especially with the circle of direct rays removed from the image. These results support that the simulation is physically valid.

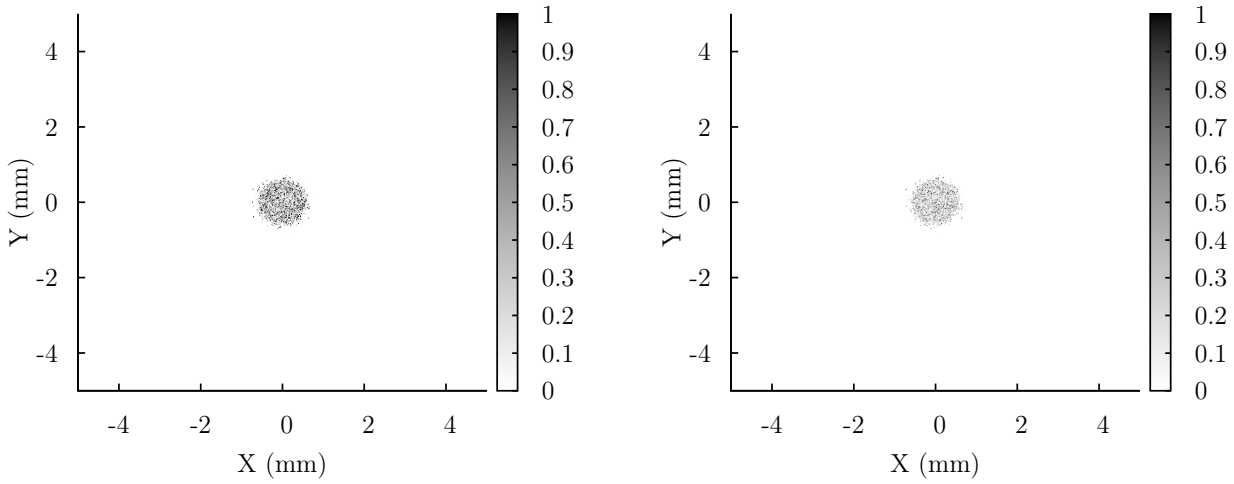

Figure 10: Spatial distributions at 1 mm with all rays included (left) and only indirect rays (right)

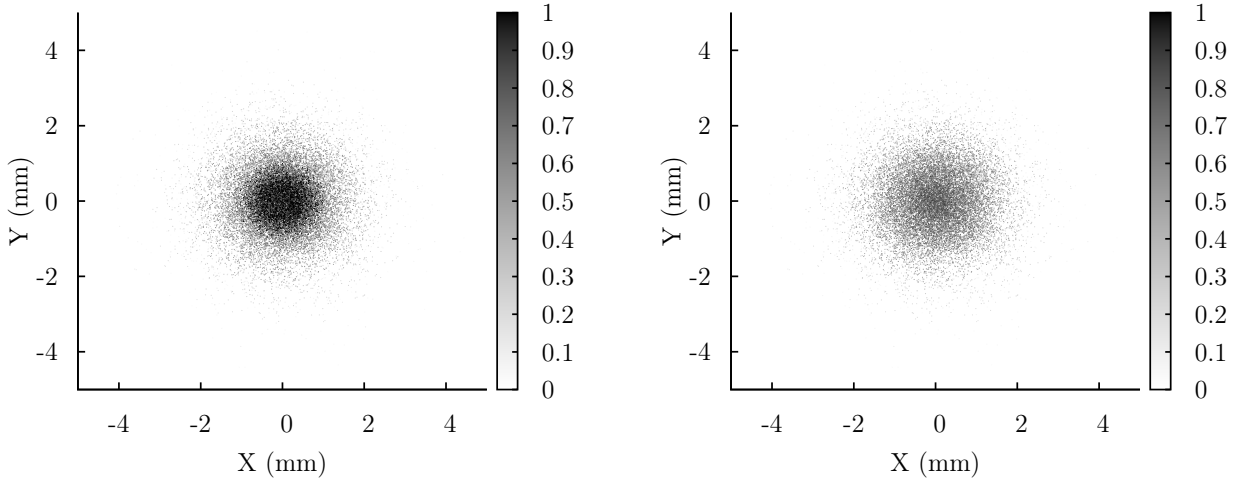

Figure 11: Spatial distributions at 10 mm with all rays included (left) and only indirect rays (right)

5 Experimental verification

The final task in the project was to confirm that the raytracer was indeed giving physical results for transmission values by testing the proposed setup, off of the capillary puller, with preexisting glass tubes. For simplicity, *straight unmodified tubes* of varying lengths from 15.2 mm to 201.3 mm had light shined through them from a UV LED powered by a regulated power supply. At the tube ends, the light passed through a 280 nm UV filter and was then collected by a photodiode. The photodiode circuit had a signal amplifier built into it that was capable of accounting for dark current and output a voltage signal based on the current being read by the diode. This voltage was recorded with a multimeter. Because the current measured in the LED could not be kept completely constant, the measured voltage readings were normalized to a single current, which constituted the transmission intensity measurements. One difficulty with this setup is that the light flux incident

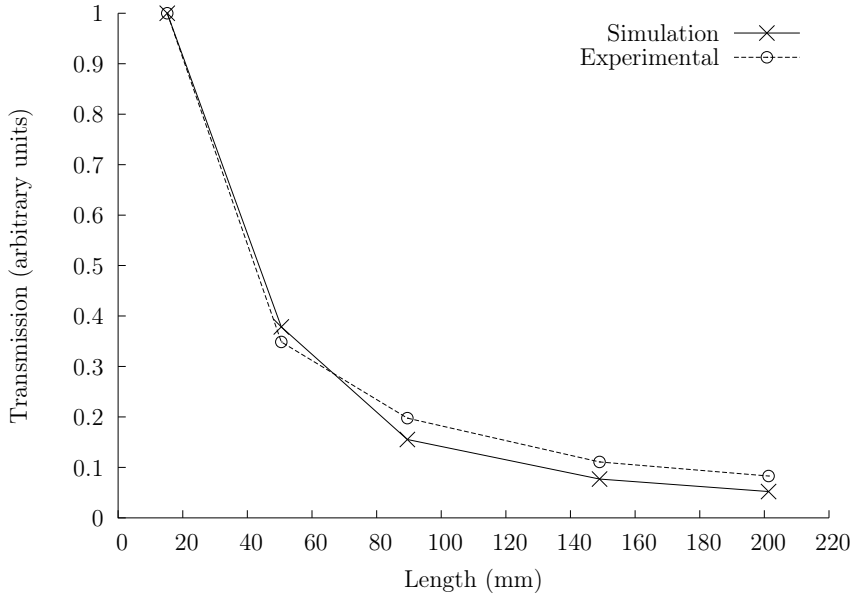

Figure 12: Simulated light transmission through a straight tube compared to experiment

on the glass tubes is unknown. Thus, while my simulations give the transmission as a ratio of the incident light, for these measurements one can only compare the values to one another without being privy to the ratios. Thus in order to compare the two, some normalization is required. The most conventional, and logical, choice is to normalize the curves based on the values given for the shortest tube; that is what has been done in Figure 12. The reasoning is due to the fact that the simulation should be most accurate for the shortest tubes because at reflection points, when the mathematics occur, is where error is introduced into the simulation. Thus more reflections, or a higher bounce number, for a ray means that the simulation accuracy of that ray is less. This is somewhat self-correcting; within a single tube, in simulation and reality the rays that bounce most often tend to be attenuated far more and thus contribute less information. However, longer tubes will have greater bounce numbers than shorter ones, and also larger error. If the error is indeed

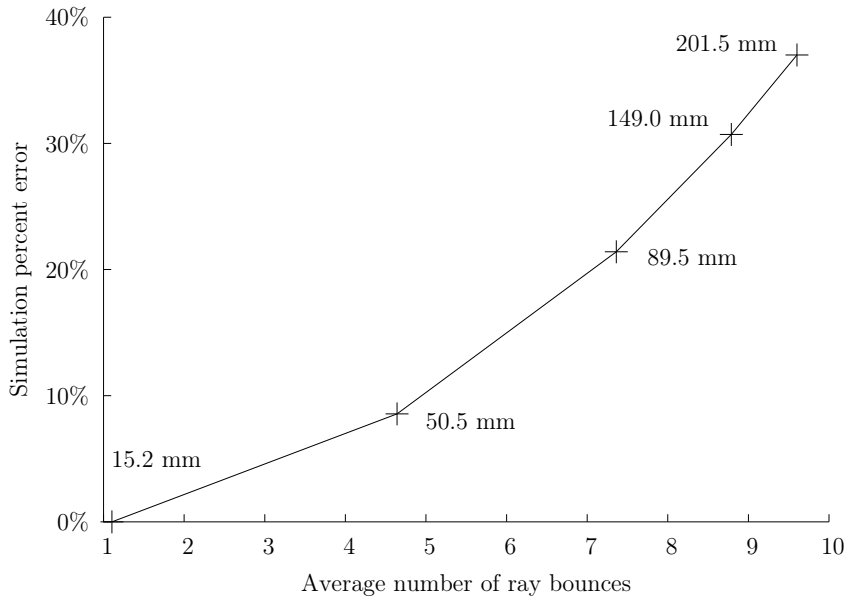

Figure 13: Percent error of simulation related to average ray bounce count per tube

tied to bounce numbers there should be a visible relationship between the two. Figure 13 gives this relationship. It appears to be mostly linear, which is to be expected, with a slight upward curvature. The fact that this curve is linear implicates the scattering amounts used in the capillary profile generation. It is very possible that too little random scattering was used, and this had a very direct linear relationship on the simulated results. The explanation for this curvature may well lie in the UV filter used in experiment. It was almost, but not entirely, opaque to the visible light emitted by the LED. The glass walls of the tubes used in the experiments trapped visible light and carried it down to the photodiode using total internal reflection, where the majority of it was filtered out. However, one could visibly confirm that some of the light was not blocked by the filter. This amount of light was relatively constant with changing tube length, and would have contributed significantly more error to the calculations of the lower-intensity (i.e., long) tubes.

Conclusion & acknowledgments

The primary product of my work is the working, versatile, three-dimensional capillary raytracer that accounts for inherent real imperfections, which Cornell did not have prior to this project. This is very important; the code can be easily adapted in the future to trace x-rays, or any other type of light, and can generate simulated far-field images from real capillary profiles as well as total intensity calculations. The vectorized, parallel methodology means that much higher ray counts can be used with slower processors and lower computation times. If used on a high-performance computing system, it would be very possible to cast tens of millions of rays within a reasonable time frame.

As for the question posed by this project's title, whether or not the new metrology is feasible, all indications are that it is. It is not sensitive to bending except possibly with very small ID capillaries paired with very large deflections; random scattering also has no effect on the measurement in question, recording transmission during the pulling process. The experimental comparison is promising, showing a very similar general shape, with errors for low-intensity tubes apparently being ascribable to a combination of experimental error due to visible light collection, and a discrepancy in the amount of random scattering (diameter error) in the initial conditions of the simulations and the actual tubes. Neither of these factors is a result of inaccuracy in the raytracing methodology.

This REU project was supported by NSF grant PHY-1156553. My advisor Dr. Rong Huang gave constant assistance and extremely helpful explanations of various simulation specifics. Dr. Peter Revesz worked on the experimental setup and provided important candid impressions of my work. Tom Szebenyi gave invaluable technical explanations of capillary pulling. Monica Wesley, Ivan Bazarov, Georg Hoffstaetter and others did a great deal of organizational work.

List of Figures

References

[1] Sterling W. Cornaby. *The handbook of x-ray single-bounce monocapillary optics, including optical design and synchrotron applications.* PhD thesis, Cornell University, 2008.

[2] R. Huang and D. H. Bilderback. Single-bounce monocapillaries for focusing synchrotron radiation: Modeling, measurements and theoretical limits. *J. Synchrotron Radiation*, 13:74–84, 2006.

[3] L. Vincze, K. Janssens, F. Adams, and A. Rindby. Detailed ray-tracing code for capillary optics. *X-ray Spectrometry*, 24:27–37, 1995.